

Accelerating Federated Learning with a Global Biased Optimiser

Jed Mills, Jia Hu, Geyong Min, Rui Jin, Siwei Zheng, Jin Wang

Department of Computer Science, University of Exeter, UK
 {jm729, j.hu, g.min, rj390, sz413, jw855}@exeter.ac.uk

Abstract

Federated Learning (FL) is a recent development in the field of machine learning that collaboratively trains models without the training data leaving client devices, in order to preserve data-privacy. In realistic settings, the total training set is distributed over clients in a highly non-Independent and Identically Distributed (non-IID) fashion, which has been shown extensively to harm FL convergence speed and final model performance. We propose a novel, generalised approach for applying adaptive optimisation techniques to FL with the Federated Global Biased Optimiser (FedGBO) algorithm. FedGBO accelerates FL by applying a set of global biased optimiser values during the local training phase of FL, which helps to reduce ‘client-drift’ from non-IID data, whilst also benefiting from adaptive momentum/learning-rate methods. We show that the FedGBO update with a generic optimiser can be viewed as a centralised update with biased gradients and optimiser update, and use this theoretical framework to prove the convergence of FedGBO using momentum-Stochastic Gradient Descent. We also perform extensive experiments using 4 realistic benchmark FL datasets and 3 popular adaptive optimisers to compare the performance of different adaptive-FL approaches, demonstrating that FedGBO has highly competitive performance considering its low communication and computation costs, and providing highly practical insights for the use of adaptive optimisation in FL.

1 Introduction

Due to increasing public concern regarding data privacy, Federated Learning (FL) is a sub-field of machine learning that aims to collaboratively train a model in a distributed fashion without the training data leaving the devices where it was generated. In real-world settings, FL deployments can range from ‘cross-device’ scenarios where huge numbers of client devices (such as smartphones) participate, to ‘cross-silo’ scenarios with fewer clients (such as institutions like hospitals) (Kairouz and McMahan 2021). As data does not leave client devices in FL, they receive a much higher degree of data-privacy compared to traditional training which would typically require clients to upload this sensitive data for centralised training in the cloud.

Preprint. Article under review.

Despite the highly attractive data-privacy benefits of FL, there exist several significant challenges to designing effective and efficient FL algorithms, especially for the cross-device scenario. These challenges include:

- **Heterogeneous client data:** as data is generated on each client device, and data shuffling is prohibited for privacy reasons, the client data is highly non-Independent and Identically Distributed (non-IID). However, ML algorithms typically assume training samples are drawn IID from the true distribution, and non-IID client data has been extensively shown to harm model convergence in FL.
- **Client networking constraints:** in the cross-device FL setting, there are a huge number of (typically wirelessly-connected) devices such as smartphones, and the bandwidth between the clients and server in FL is assumed to be scarce. On top of this, clients can connect to and disconnect from the FL process arbitrarily.
- **Long training times:** in a real-world FL deployment, client devices would have to meet criteria in order to join the FL process. For example, in previous deployments using smartphones, client devices had to be connected to the Internet and charging in order to participate in FL. Therefore, the time required to wait for clients to become available for FL training means rounds of FL would take a large amount of real-time. On top of this, client devices may have low computational power (such as embedded or IoT devices), further increasing training time.

A naive approach to distributed training for FL would be to simply use the distributed SGD algorithm: until the FL model converges, clients compute a single batch gradient and upload these gradients to the server in rounds of communication, where the server applies a single step of SGD per round. However, in practice, distributed SGD takes an incredibly larger number of communication rounds for the trained model to converge. In order to address some of the above challenges, (McMahan et al. 2017) published the *Federated Averaging* (FedAvg) algorithm. FedAvg works very similar to distributed SGD, however, clients perform multiple steps of SGD locally per communication round, before uploading their models to the server. The server averages all

uploaded client models before starting a new round.

(McMahan et al. 2017) showed that FedAvg can reduce the number of communication rounds required for the FL model to reach a given target accuracy, compared to distributed SGD. Therefore, FedAvg can be considered more communication-efficient. However, the authors also showed that increasing the number of local SGD steps performed by FedAvg gave diminishing returns at improving convergence speed, and that non-IID client data harms the convergence speed and final accuracy of the global model. Therefore, there has been much research interest in developing new FL algorithms that exhibit faster convergence (in terms of communication rounds) compared to FedAvg, and algorithms that fare better in the face of non-IID client data.

When clients perform $K > 1$ steps of SGD locally during FedAvg, the unique models that client produce move towards the minimiser of the local objective. When client data is distributed in a non-IID fashion, this causes client models to exhibit ‘client-drift’ (Karimireddy et al. 2020b): the client models move towards unique, non-identical minimisers. When client models are averaged (as in FedAvg), this average of client minimisers may *not* be the same as the minimiser that would be produced by centralised training on pooled client data. (Karimireddy et al. 2020b) proposed the SCAFFOLD algorithm to address this problem, which features local (to each client) and global control variates that are applied during local SGD. These variates reduce the impact of client drift, and the authors show on simulated datasets that SCAFFOLD is less negatively affected by larger K , and can reduce the number of rounds required to reach a target accuracy for real-world datasets. However, SCAFFOLD requires stateful clients (in order to maintain local control variates), breaking one of the requirements for the cross-device FL scenario, and also increases the per-round communication cost compared to FedAvg (due to communicating control variates).

Later, (Karimireddy et al. 2020a) proposed the Mime framework that also tackles the problem of client-drift. In Mime, a set of global optimiser statistics are tracked, and a control variate is used, reducing client-drift and improving convergence speed. These authors proved the theoretical advantages of Mime for convex and nonconvex objectives, and demonstrated its real-world performance on benchmark FL datasets. However, Mime also exhibits the limitations of increased communication and local computation cost compared to FedAvg. Other authors have also investigated ways of incorporating adaptive optimisation into FedAvg to improve convergence. (Leroy et al. 2019) and (Reddi et al. 2021) proposed adding adaptive optimisation to the server-level update of the global model: a set of global statistics are tracked, and applied to the global-model update each round. This generic algorithm does not increase communication or local computation costs compared to FedAvg, however, does not benefit from adaptive optimisation on clients. Alternatively, (Liu et al. 2020) proposed using momentum-SGD (SGDm) on clients, and averaging the momentum parameters alongside model parameters each round. Their MFL algorithm demonstrated significant speedup compared to FedAvg, but naturally increases communication and local com-

putation costs. Similarly, (Mills, Hu, and Min 2020) averaged client Adam optimiser parameters alongside model weights to improve convergence speed, along with added compression. For the rest of this work, we refer to the algorithm that keeps a set of global optimiser parameters which are averaged alongside model parameters as MFL.

Our contributions: we propose a new algorithm for FL, the Federated Global Biased Optimiser (FedGBO) algorithm. FedGBO is a generic algorithm that can be used with a variety of adaptive optimisers, designed to address the issue of client-drift in FL by keeping a set of global adaptive parameters that are applied locally (but not updated) on clients, while having lower computation and communication costs compared to competing algorithms. We show that the updates of FedGBO can be viewed as perturbed updates of a centralised optimiser, and prove the convergence of FedGBO for nonconvex objectives when using momentum-SGD. We also perform an extensive set of comparison experiments on the various recently-proposed adaptive FL methods. These experiments demonstrate that the convergence speed of FedGBO is very competitive with the other algorithms, whilst significantly reducing the communication cost of training compared to other adaptive FL algorithms. FedGBO also only slightly increases the amount of computation that clients perform per round compared to FedAvg. We also provide highly practical insights and recommendations for the use of adaptive optimisation within FL based on our thorough experimentation.

2 The FedGBO Algorithm

Algorithm 1: FedGBO

```

initial global model  $\mathbf{x}_1$ , optimiser statistics  $\mathbf{s}_1$ 
for round  $t = 1 \dots T$  do
  select round clients  $\mathcal{S}_t$ 
  for client  $i \in \mathcal{S}_t$  in parallel do
    download global model  $\mathbf{x}_t$ , statistics  $\mathbf{s}_t$ 
    initialise local model,  $\mathbf{y}_0^i \leftarrow \mathbf{x}_t$ 
    for local SGD step  $k = 1 \dots K$  do
      compute minibatch gradient  $\mathbf{g}_t^i$ 
       $\mathbf{y}_k^i \leftarrow \mathbf{y}_{k-1}^i - \eta \mathcal{U}(\mathbf{g}_t^i, \mathbf{s}_t)$ 
    end
    upload local model  $\mathbf{y}_K^i$  to server
  end
  update global model  $\mathbf{x}_{t+1} \leftarrow \frac{1}{|\mathcal{S}_t|} \sum_{i \in \mathcal{S}_t} \mathbf{y}_K^i$ 
  compute average gradient
   $\tilde{\mathbf{g}}_t \leftarrow \mathcal{I}(\mathbf{x}_t, \mathbf{x}_{t+1}, \mathbf{s}_t, K, \eta)$ 
  update global statistics  $\mathbf{s}_{t+1} \leftarrow \mathcal{T}(\tilde{\mathbf{g}}_t, \mathbf{s}_t)$ 
end

```

Federated Global Biased Optimiser (FedGBO) is a round-based FL algorithm like FedAvg and related algorithms. FedGBO aims to reduce client-drift by keeping a set of global statistics, which clients download at the start of each communication round. These global statistics are not updated during client updates, but are kept constant, as shown in Algorithm 1. When the ‘momentum’ parameter of an

Table 1: Update, Tracking and Inverse steps for popular optimisation algorithms.

Algorithm	Statistics	Update \mathcal{U}	Track \mathcal{T}	Inverse \mathcal{I}
RMSProp	\mathbf{v}	$\frac{-\eta\mathbf{g}}{\sqrt{\mathbf{v}+\epsilon}}$	$\mathbf{v} \leftarrow \beta\mathbf{v} + (1-\beta)\mathbf{g}$	$\frac{1}{\eta K}(\mathbf{x}_t - \mathbf{x}_{t+1})(\sqrt{\mathbf{v}} + \epsilon)$
SGDm	\mathbf{m}	$-\eta(\beta\mathbf{m} + (1-\beta)\mathbf{g})$	$\mathbf{m} \leftarrow \beta\mathbf{m} + (1-\beta)\mathbf{g}$	$\frac{1}{1-\beta}\left(\frac{\mathbf{x}_t - \mathbf{x}_{t+1}}{\eta K} - \beta\mathbf{m}\right)$
Adam	\mathbf{m}, \mathbf{v}	$\frac{-\eta(\beta_1\mathbf{m} + (1-\beta_1)\mathbf{g})}{\sqrt{\mathbf{v}+\epsilon}}$	$\mathbf{m} \leftarrow \beta_1\mathbf{m} + (1-\beta_1)\mathbf{g}$ $\mathbf{v} \leftarrow \beta_2\mathbf{v} + (1-\beta_2)\mathbf{g}$	$\frac{1}{1-\beta_1}\left(\frac{(\mathbf{x}_t - \mathbf{x}_{t+1})(\sqrt{\mathbf{v}} + \epsilon)}{\eta K} - \beta_1\mathbf{m}\right)$

adaptive optimiser is larger (e.g., β in SGDm), the sum of updates computed by clients will have less influence from local gradients, thus reducing the opportunity for drift. FedGBO is a generic FL algorithm that can be used with any adaptive optimiser that can be represented as an update (\mathcal{U}), tracking (\mathcal{T}) and inverse (\mathcal{I}) step. In Table 1, we present the $\mathcal{U}, \mathcal{T}, \mathcal{I}$ steps for three popular optimisers: RMSProp (Tieleman and Hinton 2012), SGDm, and Adam (Kingma and Ba 2015).

As presented in Algorithm 1, in each communication round of FedGBO, a random subset of clients are selected to participate. This selection forces partial client participation in the experimental setting, however, in a real-world deployment, clients devices will participate if they are available for training (e.g. for smartphone clients, this may be when they are charging and connected to WiFi) (Bonawitz et al. 2019).

Participating clients download the global model \mathbf{x}_t and optimiser values \mathbf{s}_t . Clients then perform K steps of adaptive optimisation using the generic update step \mathcal{U} and locally computed stochastic gradients. After local training, all participating clients upload their local models to the server. The server computes the new global model \mathbf{x}_{t+1} as an average of client models. It performs the generic inverse-step \mathcal{I} to compute the average gradient during the client local updates. The server then updates the global statistics using the generic tracking step \mathcal{T} .

An alternative implementation of FedGBO (that would not require optimisers to be represented using an inverse step \mathcal{I}) would update the local model \mathbf{y}_k^i on clients, whilst also maintaining a copy of the average local gradient (which would be the same size as the model used, $|\mathbf{x}|$). This average local gradient would then be uploaded to the server, and could be used to update the global model and global statistics instead of performing an inverse step \mathcal{I} . However, FedGBO is designed to be very lightweight in terms of computation and memory cost for clients, as real-world FL scenarios can involve very low-powered clients such as IoT devices. Therefore, our formulation decreases the memory and total computational cost for clients, as the average gradient does not have to be stored alongside \mathbf{y}_k^i .

In Section 4, we compare various algorithms that apply adaptive optimisation to FL. From an algorithmic standpoint, FedGBO has the joint-lowest upload cost among the compared algorithms ($|\mathbf{x}|$), alongside FedAvg and AdaptiveFedOpt (Reddi et al. 2021). However, we later show experimentally that the client-side adaptive optimisation used by FedGBO can achieve significant speedup compared to FedAvg and AdaptiveFedOpt, which use vanilla SGD for the local update. FedGBO therefore has the lowest up-

load cost among the algorithms that use client-side adaptive optimisation (FedGBO, MFL (Liu et al. 2020), Mimelite (Karimireddy et al. 2020a)), and does not require the potentially very expensive computation of full-batch gradients by clients (as Mimelite does). Table 2 compares these adaptive FL approaches and details their communication and memory requirements.

3 Convergence Analysis

In this section, we show that the updates to the global model in FedGBO with a generic optimiser can be formulated as updates to that same optimiser in the centralised setting, with a perturbed gradient and statistics update. We then show that this formulation can be used to extend existing convergence analyses by applying a recent analysis of SGDm (Désossez et al. 2020) to the FedGBO algorithm, recovering the same tight dependence on β as in the centralised analysis, with added client-drift terms associated with FL.

In FL, we wish to train a model $\mathbf{x} \in \mathbb{R}^d$ that minimises the following objective function:

$$F(\mathbf{x}) = \mathbb{E}_i \left[f_i(\mathbf{x}) = \frac{1}{n_i} \sum_{j=1}^{n_i} f(\mathbf{x}; \xi_{i,j}) \right], \quad (1)$$

where f_i , n_i and $\{\xi_{i,1}, \dots, \xi_{i,n_i}\}$ denote the average loss, total number of samples, and training samples on client i , respectively. f is the loss function that clients use to train \mathbf{x} . Intuitively, we wish to minimise the expected loss over all samples and over all clients, as would be minimised by training in the centralised setting over pooled data. We present the individual client losses f_i as a sum, and the global loss F as an expectation, to emphasise that in FL there are a very large number of clients, each possessing a small number of local samples.

Clients are assumed to have heterogeneous local data distributions. Therefore, the local minimisers for any two clients i and j are not necessarily the same: $f_i^* \neq f_j^*$. This is the source of client drift for $K > 1$ local updates. We make the following standard assumptions to make the analysis of FedGBO tractable:

Assumption 1 (Lower bound). F is bounded below by F^* : $F(\mathbf{x}) > F^*, \forall \mathbf{x} \in \mathbb{R}^d$.

Assumption 2 (Inter-client variance). The variance of client gradients is bounded: $\mathbb{E}_i [\|\nabla f_i(\mathbf{x}) - \nabla F(\mathbf{x})\|^2] \leq G^2, \forall i$.

Assumption 3 (Gradient magnitude). The magnitude of client gradients is bounded: $\|f_i(\mathbf{x}; \xi)\|^2 \leq R^2, \forall i$.

Table 2: Different momentum-based FL algorithms.

Algorithm	Approach	Download	Upload	∇f	Memory
FedAvg (McMahan et al. 2017)	Average client models	\mathbf{x}	\mathbf{x}	No	$\mathcal{O}(\mathbf{x})$
FedOpt (Reddi et al. 2021)	Adds server statistics	\mathbf{x}	\mathbf{x}	No	$\mathcal{O}(\mathbf{x})$
MFL (Liu et al. 2020)	Also averages statistics	\mathbf{x}, \mathbf{s}	\mathbf{x}, \mathbf{s}	No	$\mathcal{O}(\mathbf{x} + \mathbf{s})$
Mimelite (Karimireddy et al. 2020a)	Unbiased global statistics	\mathbf{x}, \mathbf{s}	$\mathbf{x}, \nabla \mathbf{f}$	Yes	$\mathcal{O}(2 \mathbf{x} + \mathbf{s})$
FedGBM (Ours)	Biased global statistics	\mathbf{x}, \mathbf{s}	\mathbf{x}	No	$\mathcal{O}(\mathbf{x} + \mathbf{s})$

Assumption 4 (Lipschitz gradients). *Client loss functions are L -smooth: $\|\nabla f_i(\mathbf{x}; \xi) - \nabla f_i(\mathbf{y}; \xi)\| \leq L\|\mathbf{x} - \mathbf{y}\|, \forall i$.*

Assumption 5 (Intra-client variance). *Client stochastic gradients are unbiased estimates of the local gradients, $\mathbb{E}_{\xi}[\nabla f_i(\mathbf{x}; \xi)] = \nabla f_i(\mathbf{x}), \forall i$, with bounded variance: $\mathbb{E}_{\xi}[\|\nabla f_i(\mathbf{x}; \xi) - \nabla f_i(\mathbf{x})\|^2] \leq \sigma^2, \forall i$.*

As F is a convex combination of client objective functions f_i , F is therefore also L -smooth.

Previously, (Karimireddy et al. 2020a) showed that FedAvg with $K > 1$ local updates could be reformulated as centralised optimisation, with a perturbed gradient, which they then use to prove the convergence of their Mime algorithm. The perturbation, \mathbf{e}_t of the centralised-training gradient \mathbf{g}_t is defined as:

$$\mathbf{e}_t = \frac{1}{KS} \sum_{i=1}^K \sum_{i \in S} (\nabla f_i(\mathbf{y}_{i,k-1}; \xi_{i,k}) - \nabla f_i(\mathbf{x}; \xi_{i,k})), \quad (2)$$

for local iterations $\{y_{i,0}, \dots, y_{i,K-1}\}$, total number of local iterations K , and total number of sampled clients S . Thus, the gradient-perturbation \mathbf{e}_t is the average difference in gradients over the K local steps and S clients, to the gradients that would have been computed using the global model. Using this definition, we can rewrite the updates of FedGBO as perturbed updates to a centralised optimiser:

$$\begin{aligned} \mathbf{x}_t &\leftarrow \mathbf{x}_{t-1} - \tilde{\eta} \mathcal{U}(\mathbf{g}_t + \mathbf{e}_t, \mathbf{s}_{t-1}), \\ \mathbf{s}_t &\leftarrow \mathcal{V}(\mathbf{g}_t + \mathbf{e}_t, \mathbf{s}_{t-1}), \end{aligned}$$

for generic model-update step \mathcal{U} and optimiser statistics tracking step \mathcal{T} , and ‘psuedo-learning-rate’ $\tilde{\eta} = K\eta$. The local updates of FedGBO use fixed global statistics, in a similar manner to the fixed statistics used in Mime (albeit we used biased global statistics). As we make assumptions at least as strong as those from (Karimireddy et al. 2020a), we can directly use their result to bound the norm of the perturbation \mathbf{e}_t :

$$\mathbb{E}_t[\|\mathbf{e}_t\|^2] \leq (B^2 L^2 \tilde{\eta}^2) \left(\mathbb{E}_t[\|\mathbf{g}_t\|^2] + G^2 + \frac{\sigma^2}{K} \right), \quad (3)$$

where $B \geq 0$ is a bound on the Lipschitzness of the optimiser \mathcal{U} ’s update: $\|\mathcal{U}(\mathbf{g})\| \leq B\|\mathbf{g}\|$.

Using the perturbed gradient and momentum generalisation presented above, updates of FedGBO using the specific

SGDm optimiser can be written as:

$$\mathbf{m}_t \leftarrow \beta \mathbf{m}_{t-1} + (\mathbf{g}_{t-1} + \mathbf{e}_{t-1}) \quad (4)$$

$$\mathbf{x}_t \leftarrow \mathbf{x}_{t-1} - \tilde{\eta} \mathbf{m}_t. \quad (5)$$

While the specific SGDm implementation we use in the later experiments multiplies the second term of (4) by a $(1 - \beta)$ term (we find hyperparameter choice with this implementation tends to be more intuitive), we drop the $(1 - \beta)$ term from (4) in order to simplify the proof, and assume the $(1 - \beta)$ and β terms can be incorporated into $\tilde{\eta}$. As is typical for nonconvex analysis, we now bound the expected squared norm of the model gradient at communication round t . For total iterations T , we define t as a random index with value $\{0, \dots, T - 1\}$, with probability distribution $\mathbb{P}[t = j] \propto 1 - \beta^{T-j}$. Full proofs are given in Appendix A.

Theorem 1 (Convergence of FedGBO using SGDm) *Let the assumptions A1-A5 hold, the total number of iterations $T > (1 - \beta)^{-1}$, $\tilde{\eta} = K\eta > 0, 0 \leq \beta < 1$, and using the update steps given by (4) and (5).*

$$\begin{aligned} \mathbb{E}[\|\nabla F(\mathbf{x}_t)\|^2] &\leq \frac{2(1 - \beta)}{\tilde{\eta} \tilde{T}} (F(\mathbf{x}_0) - F^*) + \frac{TZ}{\tilde{T}} \\ &\quad + \frac{2T\tilde{\eta}L(1 + \beta)(R^2 + Z)}{\tilde{T}(1 - \beta)}, \quad (6) \end{aligned}$$

where $\tilde{T} = T - \frac{\beta}{1 - \beta}$, and $Z = 18B^2 L^2 \tilde{\eta}^2 \left(R^2 + G^2 + \frac{\sigma^2}{K} \right)$.

Theorem 1 therefore shows that the perturbed gradient and momentum framework presented above can be used to apply an existing convergence proof from an optimiser in the centralised setting to the FedGBO framework. Next, we simplify Theorem 1 to achieve a more explicit convergence rate.

Corollary 1 (Theorem 1 simplification using iteration assumption) *Making the same assumptions as in Theorem 1, and also that $N \gg (1 - \beta)^{-1}$, hence $\tilde{T} \approx T$, and using $\tilde{\eta} = (1 - \beta) \frac{2C}{\sqrt{T}}$, for $C > 0$, then*

$$\begin{aligned} \mathbb{E}[\|\nabla F(\mathbf{x}_t)\|^2] &\leq \frac{1}{C\sqrt{T}} (F(\mathbf{x}_0) - F^*) + Z \\ &\quad + \frac{4CL(1 + \beta)(R^2 + Z)}{\sqrt{T}(1 - \beta)}. \quad (7) \end{aligned}$$

Table 3: Details of experimental tasks presented in Section 4 (CNN = Convolutional Neural Network, GRU = Gated Recurrent Network).

Task	Type	Classes	Model	Total Clients	Sampled Clients per Round	Mean Samples per Client
CIFAR100	Image classification	100	CNN	500	5	100
Sent140	Sentiment analysis	2	Linear	21876	22	15
FEMNIST	Image classification	62	CNN	3000	30	170
Shakespeare	Next-character prediction	79	GRU	660	7	5573

Corollary 1 shows that we can recover the same $\mathcal{O}(\frac{1}{\sqrt{T}})$ convergence rate that (Défosses et al. 2020) achieved in the centralised setting, with some modified constants and with an added error term. Specifically, the Z in the third term of (7) arises from using biased momentum, and it is also decreased with $\mathcal{O}(\frac{1}{\sqrt{T}})$. The second term in (7) does not decrease with increasing iterations, however, and is only improved by reducing the pseudo-learning rate $\tilde{\eta}$. This second term is due to a combination of client-drift, and stochastic gradients computed on clients, and as has been noted in previous works (Karimireddy et al. 2020b) (Karimireddy et al. 2020a) (Li et al. 2020), suggests that either the learning rate η or number of local iterations K should be decayed during training to converge arbitrarily close to the stationary point.

4 Experiments

In this section, we conduct a comprehensive comparison between various state-of-the-art algorithms that incorporate adaptive optimisation into FL (including the proposed FedGBO algorithm). The experiments are conducted on 4 benchmark FL datasets, from the learning domains of image classification, sentiment analysis, and language modelling. Each adaptive FL algorithm is generic in the adaptive optimiser used, so we test three of the most popular and ubiquitous optimisers: RMSProp (Tieleman and Hinton 2012), SGDm and Adam (Kingma and Ba 2015). Table 3 gives a brief overview of the FL datasets and models used, with more thorough details given in Appendix B.

4.1 Convergence Speed

We first compare the convergence speed of the different adaptive FL algorithms using each optimiser, on each dataset. For each [dataset, FL algorithm, optimiser] combination, we tuned hyperparameters via grid search in order to achieve the highest test-set accuracy within 5,000 communication rounds. We tested learning rates in the range $\eta \in [10^1, 10^{-5}]$, with step size of 0.1, and optimiser parameter $\beta = \{0.3, 0.6, 0.9, 0.99, 0.999, 0.9999\}$. For Adam, in order to keep the number of experiments performed feasible, we fixed $\beta_2 = 0.99$ for all experiments and tuned β_1 as above. For RMSProp and Adam, as has been noted previously for adaptive FL algorithms (Reddi et al. 2021) (Karimireddy et al. 2020a), we found that a large adaptivity parameter $\epsilon = 10^{-3}$ was required for stable convergence. For the AdaptiveFedOpt algorithm, we also tested the local learning rate η_l with the same values as η . Tuning the AdaptiveFedOpt algorithm took therefore significantly more simulations compared to the other algorithms, due to the extra

hyperparameter, which represents a drawback for the practical use of AdaptiveFedOpt. For FedAvg, we tune only η , and present the same curve in each column of Figure 1. Further details about experimental settings and the specific hyperparameters used are given in Appendix B.

Figure 1 presents the test-set accuracies during training for these tuned parameters, for $K = 10$ local steps. We consider this a ‘low- K ’ regime, representing scenarios where clients can communicate more frequently with the server.

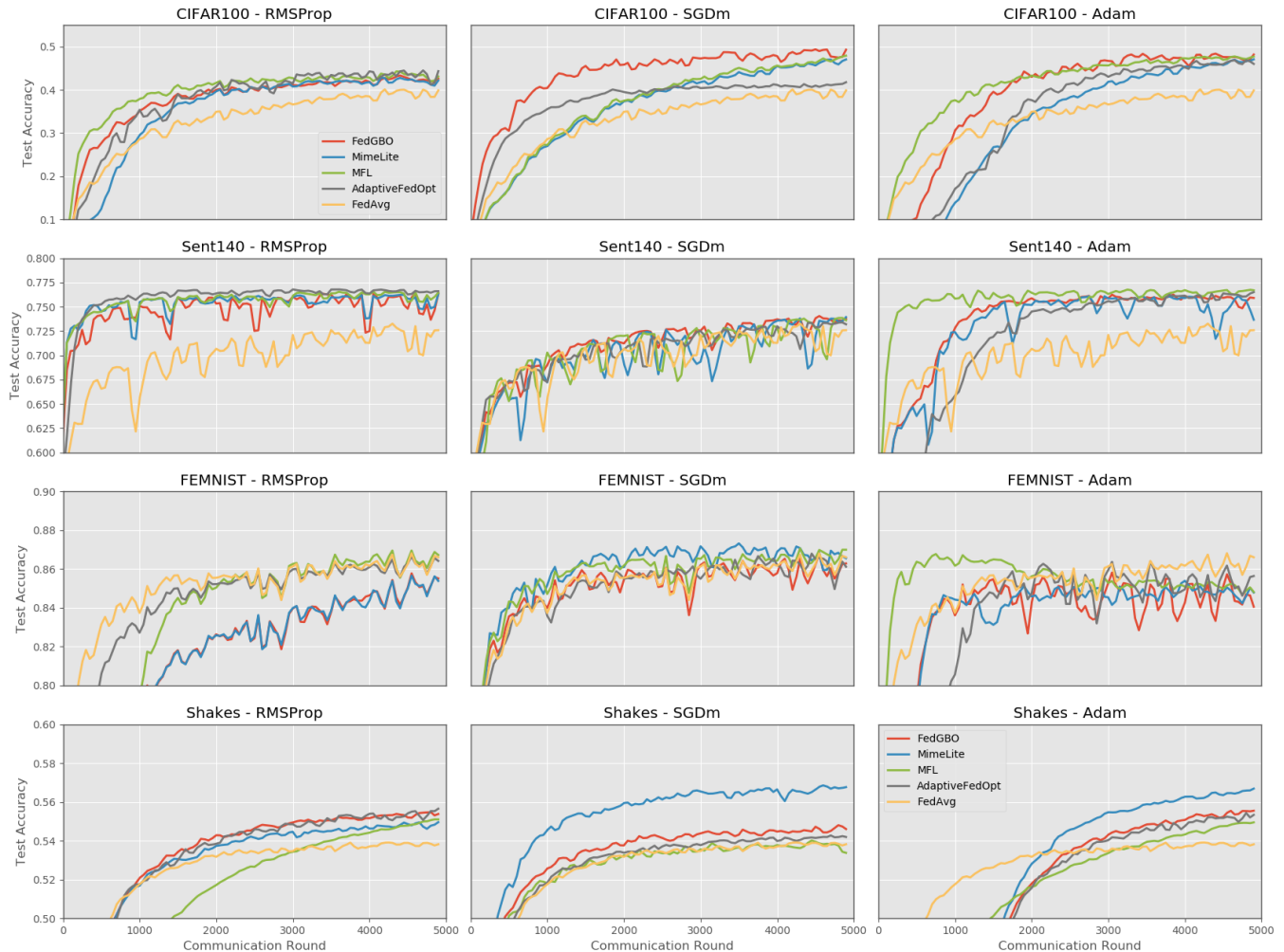
Choice of FL algorithm. Comparing the rows of Figure 1, there is no clear FL algorithm that has universally superior performance in terms of convergence speed. For the CIFAR100 dataset, FedGBO with SGDm converges fastest, whereas for the Shakespeare dataset Mimelite with SGDm converges fastest. However, for the FEMNIST dataset, the adaptive FL algorithms provide little benefit over FedAvg. The reason for this result with FEMNIST is likely because it is a relatively simple greyscale task, so there is little benefit to be had by using adaptive optimisation.

Therefore, when planning a real-world FL deployment, the potential benefit of adaptive algorithms should be taken into account. If the learning task is relatively simple, the additional hyperparameters (which then need to be tuned) that adaptive FL algorithms add may outweigh the little performance gain over FedAvg with fewer hyperparameters. Conversely, on the much more challenging CIFAR100 image classification task, the adaptive FL algorithms provide significant speedup compared to FedAvg.

Alongside this, the communication costs of the various adaptive FL algorithms should be taken into account. AdaptiveFedOpt does not add to the communication overhead compared to FedAvg, but adds one extra hyperparameter (η_l) to search over, on top of optimiser parameters. MFL and Mimelite both increase the downstream and upstream communication cost compared to FedAvg, while FedGBO increases only the downstream communication cost. FedGBO therefore presents a good balance between convergence speed, communication cost, and total hyperparameters: it has highly comparable performance compared to other algorithms that use client-side adaptive optimisation (MFL, Mimelite), without increasing the upload cost compared to FedAvg, and without adding extra hyperparameters to tune, as AdaptiveFedOpt does.

Choice of optimiser. As shown in Figure 1, there was also no universally-best optimiser for each dataset and adaptive FL algorithm, as is seen in centralised training. For example, the fastest convergence for Shakespeare was seen

Figure 1: Comparison of momentum-based FL algorithms on different FL datasets, using $K = 10$ local update steps.



with SGDm, whereas the fastest convergence for Sent140 was seen with RMSProp and Adam, while SGDm gave no improvement over FedAvg. The gradients computed in the Sent140 task are sparse (due to very sparse features). Adaptive learning-rate methods like RMSProp and Adam are well known to provide good convergence speed for sparse-gradient tasks. The other 3 tasks, on the other hand, do not have sparse features, and RMSProp performed largely the worst for these tasks. Therefore, these results suggest that when choosing an adaptive FL optimiser, a good initial choice of optimiser is the one that would work best on the task in the standard centralised setting. Also, as shown in Table 2, the choice of optimiser impacts the communication cost for FedGBO, MFL and MimeLite: for RMSProp and SGDm, the total download costs are doubled, and for Adam, they are tripled.

4.2 Computational Cost

Another important consideration when comparing adaptive FL algorithms, alongside convergence speed and communi-

cation cost, is computational cost of training. In cross-device FL, clients can be a highly heterogeneous set of physical devices, and the same federation may have clients with a wide range of computational power (e.g. different generations of smartphones, or clients that are resource-constrained IoT devices) (Kairouz and McMahan 2021). This has two practical implications: the time taken to perform the local training loop of the adaptive FL algorithms may represent the bottleneck in terms of training time, and FL deployments that drop stragglers (Bonawitz et al. 2019) may end up regularly dropping the same, low-powered clients each round, skewing the global model in favour of faster clients. Furthermore, recent research indicates the total energy consumed by clients during FL can exceed the energy used by centralised training, motivating development of FL algorithms that are computationally (and hence energy) cheap (Qiu et al. 2020).

Table 4 shows the total number of Floating Point Operations (FLOPs) required on average for the local update of each FL algorithm for $K = 10$ local steps. The total FLOPs for each algorithm was calculated as the sum of FLOPs re-

quired to compute K minibatch gradients (Hernandez and Brown 2020) and update the local model using any adaptive optimiser K times, plus the FLOPs required to compute full-batch gradients for Mimelite. We do not consider the computational cost of server updates here, because the server would represent a negligible proportion of total computational cost (considering there are thousands to millions of clients). We also only calculate FLOPs from an algorithmic standpoint, and do not consider optimisations such as vectorised functions, as these are reliant on specific client hardware. See Appendix B for full details about how the Table 4 values were calculated.

As shown in Table 4, the FedAvg and AdaptiveFedOpt algorithms have joint lowest FLOPs because no adaptive optimisation (only vanilla SGD) is used on clients. FedGBO has a small increase over these two schemes because clients need to incorporate gradients into the (fixed) adaptive parameters for each of the K local updates. However, this extra computational burden is small because the number of parameters in the tested models is significantly smaller than the number of operations required for a forward/backward pass. The MFL algorithm has a slightly higher computational cost compared to FedGBO for the RMSProp and Adam optimisers, because the update rule of the adaptive-gradient methods cannot be incorporated into the model update (see Appendix B). For each dataset, the Mimelite algorithm has a significantly higher computational cost because of the need to compute full-batch gradients. This is especially notable for the Shakespeare dataset, where the average number of samples per client is over 5000 (see Table 3). In our simulations (performed on GPU-equipped workstations), the Mimelite algorithm took significantly longer real-time to complete 5000 communication rounds, due to the extra computation.

Table 4: Total average FLOPs ($\times 10^8$) performed per client per round for different FL tasks, using different optimisers and FL algorithms: FedGBM, Mimelite, MFL using RMSProp, SGDm and Adam. AdaptiveFedOpt and FedAvg use SGD. Values shown for $K = 10$ local update steps, to 3 significant figures.

Task	RMSProp	SGDm	Adam	SGD
CIFAR100	50.1	50.1	50.4	49.8
	65.6	65.6	65.9	
	50.1	50.4	50.8	
Sent140	0.0280	0.0280	0.0310	0.0260
	0.0325	0.0325	0.0355	
	0.0280	0.0310	0.0340	
FEMNIST	32.1	32.1	32.3	31.9
	48.9	48.9	49.2	
	32.1	32.3	32.6	
Shakespeare	118	118	118	118
	2180	2180	2180	
	118	118	118	

Using adaptive optimisation therefore does not, *per se*, lead to a substantial increase in the computational cost of adaptive FL algorithms. Considering Figure 1, there are few

instances where FL algorithms using local adaptive optimisation (FedGBO, MFL, Mimelite) perform worse than FedAvg or AdaptiveFedOpt. Therefore for a practical FL deployment, we would suggest the computational cost of using adaptive optimisation on clients is of lesser concern when using FedGBO or MFL, especially when using small-medium sized models as are used in this paper. If Mimelite is chosen, FL organisers should be wary of clients with large numbers of local samples. A practical improvement to Mimelite might consider limiting the number of samples over which the unbiased gradients are calculated.

5 Conclusion

In this work, we proposed a new algorithm: Federated learning with Global Biased Optimiser (FedGBO) that incorporates a set of global statistics for a generic machine learning optimiser within the Federated Learning (FL) process in a novel way. FedGBO demonstrates faster convergence rates compared to FL algorithms that only use vanilla SGD on clients (such as Federated Averaging), whilst having comparatively lower communication and computation costs compared to competing FL algorithms that also use adaptive optimisation. We showed that FedGBO with a generic optimiser can be formulated as centralised training using a perturbed gradient and optimiser update, allowing analysis of generic centralised optimisers to be extended to the FedGBO algorithm. We demonstrate how similar convergence guarantees can be achieved for FedGBO compared to the centralised bounds, by applying a recent analysis of momentum-SGD to FedGBO, recovering the same bound, plus additional terms related to ‘client drift’ in FL. We then performed an extensive set of comparison experiments using 4 competing FL algorithms (3 of which also use adaptive optimisation), 3 different optimisers, and on 4 benchmark FL datasets. These experiments highlighted FedGBO’s highly competitive performance, especially considering FedGBO’s low computation and communication costs.

References

- [Bonawitz et al. 2019] Bonawitz, K. A.; Eichner, H.; Grieskamp, W.; Huba, D.; Ingerman, A.; Ivanov, V.; Kiddon, C. M.; Konečný, J.; Mazzocchi, S.; McMahan, B.; Overveldt, T. V.; Petrou, D.; Ramage, D.; and Roselander, J. 2019. Towards federated learning at scale: System design. In *SysML 2019*. To appear.
- [Caldas et al. 2019] Caldas, S.; Wu, P.; Li, T.; Konečný, J.; McMahan, H. B.; Smith, V.; and Talwalkar, A. 2019. Leaf: A benchmark for federated settings. In *NeurIPS Workshop on Federated Learning for Data Privacy and Confidentiality*.
- [Défossez et al. 2020] Défossez, A.; Bottou, L.; Bach, F.; and Usunier, N. 2020. A simple convergence proof of adam and adagrad. *arXiv e-prints arXiv:2003.02395*.
- [Hernandez and Brown 2020] Hernandez, D., and Brown, T. B. 2020. Measuring the algorithmic efficiency of neural networks. *arXiv e-prints arXiv:2005.04305*.
- [Kairouz and McMahan 2021] Kairouz, P., and McMahan, H. B. 2021. Advances and open problems in federated learning. *Foundations and Trends in Machine Learning* 14(1).
- [Karimireddy et al. 2020a] Karimireddy, S. P.; Jaggi, M.; Kale, S.; Mohri, M.; Reddi, S. J.; Stich, S. U.; and Suresh, A. T. 2020a. Mime: Mimicking centralized stochastic algorithms in federated learning. *arXiv e-prints arXiv:2008.03606*.
- [Karimireddy et al. 2020b] Karimireddy, S. P.; Kale, S.; Mohri, M.; Reddi, S.; Stich, S.; and Suresh, A. T. 2020b. SCAFFOLD: Stochastic controlled averaging for federated learning. In *Proceedings of the 37th International Conference on Machine Learning*, volume 119 of *Proceedings of Machine Learning Research*, 5132–5143. PMLR.
- [Kingma and Ba 2015] Kingma, D. P., and Ba, J. 2015. Adam: A method for stochastic optimization. In *International Conference on Learning Representations ICLR*.
- [Leroy et al. 2019] Leroy, D.; Coucke, A.; Lavril, T.; Gisselbrecht, T.; and Dureau, J. 2019. Federated learning for keyword spotting. In *IEEE International Conference on Acoustics, Speech and Signal Processing*, 6341–6345.
- [Li et al. 2020] Li, X.; Huang, K.; Yang, W.; Wang, S.; and Zhang, Z. 2020. On the convergence of fedavg on non-iid data. In *International Conference on Learning Representations*.
- [Liu et al. 2020] Liu, W.; Chen, L.; Chen, Y.; and Zhang, W. 2020. Accelerating Federated Learning via Momentum Gradient Descent. *IEEE Transactions on Parallel and Distributed Systems* 31(8):1754–1766.
- [McMahan et al. 2017] McMahan, B.; Moore, E.; Ramage, D.; and y Arcas, B. A. 2017. Communication-efficient learning of deep networks from decentralized data. *20th International Conference on Artificial Intelligence and Statistics*.
- [Mills, Hu, and Min 2020] Mills, J.; Hu, J.; and Min, G. 2020. Communication-efficient federated learning for wireless edge intelligence in iot. *IEEE Internet of Things Journal* 7(7):5986–5994.
- [Qiu et al. 2020] Qiu, X.; Parcollet, T.; Beutel, D. J.; Topal, T.; Mathur, A.; and Lane, N. D. 2020. Can federated learning save the planet? In *NeurIPS - Tackling Climate Change with Machine Learning*.
- [Reddi et al. 2021] Reddi, S. J.; Charles, Z.; Zaheer, M.; Garrett, Z.; Rush, K.; Konečný, J.; Kumar, S.; and McMahan, H. B. 2021. Adaptive federated optimization. In *International Conference on Learning Representations*.
- [Tieleman and Hinton 2012] Tieleman, T., and Hinton, G. 2012. Rmsprop, coursera: Neural networks for machine learning. *Technical Report*.

A Proofs of Theorems

In the poofs below, unless otherwise specified, the expectation $\mathbb{E}[\cdot]$ is over both the clients samples randomly in each round of FedGBO, and the random sampling of minibatches in local updates.

Lemma 1 (Bounding the momentum term). *Given $\tilde{\eta} = \eta K > 0$, $0 \leq \beta < 1$, \mathbf{m}_t defined in (4) and (5), and Assumptions A1-A5, then*

$$\mathbb{E} [\|\mathbf{m}_t\|^2] \leq 2 \frac{R^2 + Z}{(1 - \beta)^2},$$

where $Z = 18B^2L^2\tilde{\eta}^2 \left(R^2 + G^2 + \frac{\sigma^2}{K} \right)$.

Proof. Taking any iteration t :

$$\begin{aligned} \mathbb{E} [\|\mathbf{m}_t\|^2] &= \mathbb{E} \left[\left\| \sum_{i=0}^{t-1} \beta^i (\mathbf{g}_{t-i} + \mathbf{e}_{t-i}) \right\|^2 \right] \\ &\leq \left(\sum_{i=0}^{t-1} \beta^i \right) \sum_{i=0}^{t-1} \beta^i \mathbb{E} [\|\mathbf{g}_{t-i} + \mathbf{e}_{t-i}\|^2] \\ &\leq \frac{1}{1 - \beta} \sum_{i=0}^{t-1} \beta^i \mathbb{E} [\|\mathbf{g}_{t-i} + \mathbf{e}_{t-i}\|^2] \\ &\leq \frac{2}{1 - \beta} \sum_{i=0}^{t-1} \beta^i (\mathbb{E} [\|\mathbf{g}_{t-i}\|^2] + \mathbb{E} [\|\mathbf{e}_{t-i}\|^2]) \\ &\leq 2 \frac{\mathbb{E} [\|\mathbf{g}_{t-i}\|^2] + \mathbb{E} [\|\mathbf{e}_{t-i}\|^2]}{(1 - \beta)^2} \\ &\leq 2 \frac{R^2 + Z}{(1 - \beta)^2}. \end{aligned} \quad \square$$

Here, the first inequality comes from Jensen, the third inequality is from Cauchy-Schwarz and the linearity of expectation, and the last inequality from Assumption 3, and our definition of Z .

Lemma 2 (bounding the negative term of the descent lemma (16)). *Given $\tilde{\eta} = \eta K > 0$, $0 \leq \beta < 1$, \mathbf{m}_t defined in (4) and (5), and Assumptions A1-A5, then*

$$\mathbb{E}[\nabla F(\mathbf{x}_{t-1})^\top \mathbf{m}_t] \geq \frac{1}{2} \sum_{k=0}^{t-1} \beta^k \mathbb{E} [\|\nabla F(\mathbf{x}_{t-k-1})\|^2] - \frac{Z}{2(1 - \beta)} - \frac{2\tilde{\eta}L\beta(R^2 + Z)}{(1 - \beta)^3}.$$

where $Z = 18B^2L^2\tilde{\eta}^2 \left(R^2 + G^2 + \frac{\sigma^2}{K} \right)$.

Proof. To ease notation, we denote $\mathbf{G}_t = \nabla F(\mathbf{x}_{t-1})$ and $\mathbf{c}_t = \mathbf{g}_t + \mathbf{e}_t$:

$$\begin{aligned} \mathbf{G}_t^\top \mathbf{m}_t &= \sum_{k=0}^{t-1} \beta^k \mathbf{G}_t^\top \mathbf{c}_t \\ &= \sum_{k=0}^{t-1} \beta^k \mathbf{G}_{t-k}^\top \mathbf{c}_t + \sum_{k=0}^{t-1} \beta^k (\mathbf{G}_t - \mathbf{G}_{t-k})^\top \mathbf{c}_t. \end{aligned} \quad (8)$$

Due to F being L -smooth (Assumption 4), and using the relaxed triangle inequality:

$$\begin{aligned} \|\mathbf{G}_t - \mathbf{G}_{t-k}\|^2 &\leq L^2 \left\| \sum_{l=1}^k \tilde{\eta} \mathbf{m}_{n-l} \right\|^2 \\ &\leq \tilde{\eta}^2 L^2 k \sum_{l=1}^k \|\mathbf{m}_{n-l}\|^2. \end{aligned} \quad (9)$$

Using $(\lambda \mathbf{x} - \mathbf{y})^2 \geq 0, \forall \mathbf{x}, \mathbf{y} \in \mathbb{R}^d, \lambda > 0$, and hence $\|\mathbf{x}\mathbf{y}\| \leq \frac{\lambda}{2}\|\mathbf{x}\|^2 + \frac{1}{2\lambda}\|\mathbf{y}\|^2$, we can use $\mathbf{x} = \mathbf{G}_t - \mathbf{G}_{t-k}, \mathbf{y} = \mathbf{c}_t$, $\lambda = \frac{1-\beta}{k\tilde{\eta}L}$, and substitute this inequality into (8):

$$\mathbf{G}_t^\top \mathbf{m}_t \geq \sum_{k=0}^{t-1} \beta^k \mathbf{G}_{t-k}^\top \mathbf{c}_{t-k} - \sum_{k=1}^{t-1} \frac{\beta^k}{2} \left(\left((1-\beta)\tilde{\eta}L \sum_{l=1}^k \|\mathbf{m}_{t-l}\|^2 \right) + \frac{\tilde{\eta}Lk}{1-\beta} \|\mathbf{c}_{t-k}\|^2 \right).$$

Taking the expectation of both sides gives:

$$\mathbb{E}[\mathbf{G}_t^\top \mathbf{m}_t] \geq \sum_{k=0}^{t-1} \beta^k \mathbb{E}[\mathbf{G}_{t-k}^\top \mathbf{c}_{t-k}] - \tilde{\eta}L \sum_{k=1}^{t-1} \frac{\beta^k}{2} \left(\left((1-\beta) \sum_{l=1}^k \mathbb{E}[\|\mathbf{m}_{t-l}\|^2] \right) + \frac{k}{1-\beta} \mathbb{E}[\|\mathbf{c}_{t-k}\|^2] \right). \quad (10)$$

Bounding the $\mathbb{E}[\mathbf{G}_{t-k}^\top \mathbf{c}_{t-k}]$ term, this time using $(\mathbf{G}_{t-k}^\top + \mathbf{e}_{t-k})^2 \geq 0$, and hence $\mathbf{G}_{t-k}^\top \mathbf{e}_{t-k} \geq -\frac{1}{2}(\|\mathbf{G}_{t-k}\|^2 + \|\mathbf{e}_{t-k}\|^2)$, and linearity of expectation:

$$\begin{aligned} \mathbb{E}[\mathbf{G}_{t-k}^\top \mathbf{c}_{t-k}] &= \mathbb{E}[\mathbf{G}_{t-k}^\top (\mathbf{g}_{t-k} + \mathbf{e}_{t-k})] \\ &= \mathbb{E}[\mathbf{G}_{t-k}^\top \mathbf{g}_{t-k}] + \mathbb{E}[\mathbf{G}_{t-k}^\top \mathbf{e}_{t-k}] \\ &\geq \mathbb{E}[\|\mathbf{G}_{t-k}\|^2] - \frac{1}{2} \mathbb{E}[\|\mathbf{G}_{t-k}\|^2 + \|\mathbf{e}_{t-k}\|^2] \\ &= \frac{1}{2} (\mathbb{E}[\|\mathbf{G}_{t-k}\|^2] - \mathbb{E}[\|\mathbf{e}_{t-k}\|^2]). \end{aligned} \quad (11)$$

Using Cauchy-Schwarz, linearity of expectation, Assumption 3 and the definition of Z :

$$\begin{aligned} \mathbb{E}[\|\mathbf{c}_{t-k}\|^2] &= \mathbb{E}[\|\mathbf{g}_{t-k} + \mathbf{e}_{t-k}\|^2] \\ &\leq 2(\mathbb{E}[\|\mathbf{g}_{t-k}\|^2] + \mathbb{E}[\|\mathbf{e}_{t-k}\|^2]) \\ &\leq 2(R^2 + Z). \end{aligned} \quad (12)$$

Then inserting Lemma 1, (11) and (12) into (10) gives:

$$\begin{aligned} \mathbb{E}[\mathbf{G}_t^\top \mathbf{m}_t] &\geq \sum_{k=0}^t \frac{\beta^k}{2} (\mathbb{E}[\|\mathbf{G}_{t-k}\|^2] - \mathbb{E}[\|\mathbf{e}_{t-k}\|^2]) - \tilde{\eta}L \sum_{k=1}^{t-1} \frac{\beta^k}{2} \left(\left((1-\beta) \sum_{l=1}^k 2 \frac{R^2 + Z}{(1-\beta)^2} \right) + \frac{k}{1-\beta} 2(R^2 + Z) \right) \\ &= \sum_{k=0}^t \frac{\beta^k}{2} \mathbb{E}[\|\mathbf{G}_{t-k}\|^2] - \sum_{k=0}^t \frac{\beta^k}{2} \mathbb{E}[\|\mathbf{e}_{t-k}\|^2] - \tilde{\eta}L(R^2 + Z) \sum_{k=1}^{t-1} \beta^k \left(\left(\sum_{l=1}^k \frac{1}{(1-\beta)} \right) + \frac{k}{1-\beta} \right) \\ &= \sum_{k=0}^t \frac{\beta^k}{2} \mathbb{E}[\|\mathbf{G}_{t-k}\|^2] - \frac{Z}{2(1-\beta)} - \frac{2\tilde{\eta}L}{1-\beta} (R^2 + Z) \sum_{k=1}^{t-1} \beta^k k. \end{aligned} \quad (13)$$

Using Lemma B.2 from [2], which states that, for $0 < a < 1, i \in \mathbb{N}, Q \geq i$:

$$\sum_{q=i}^Q a^q q \leq \frac{a}{(1-a)^2}, \quad (14)$$

then (13) becomes:

$$\mathbb{E}[\mathbf{G}_t^\top \mathbf{m}_t] \geq \frac{1}{2} \sum_{k=0}^{t-1} \beta^k \mathbb{E}[\|\mathbf{G}_{t-k}\|^2] - \frac{Z}{2(1-\beta)} - \frac{2\tilde{\eta}L\beta(R^2 + Z)}{(1-\beta)^3}. \quad (15)$$

Substituting the definition of \mathbf{G}_t completes the lemma. \square

Theorem 1 (Convergence of FedGBO using SGDm) *Let the assumptions A1-A5 hold., the total number of iterations $T > (1-\beta)^{-1}$, $\tilde{\eta} = K\eta > 0, 0 \leq \beta < 1$, and using the update steps given by (4) and (5).*

$$\mathbb{E}[\|\nabla F(\mathbf{x}_t)\|^2] \leq \frac{2(1-\beta)}{\tilde{\eta}\tilde{T}} (F(\mathbf{x}_0) - F^*) + \frac{TZ}{\tilde{T}} + \frac{2T\tilde{\eta}L(1+\beta)(R^2 + Z)}{\tilde{T}(1-\beta)}.$$

where $\tilde{T} = T - \frac{\beta}{1-\beta}$, and $Z = 18B^2L^2\tilde{\eta}^2 \left(R^2 + G^2 + \frac{\sigma^2}{K} \right)$.

Proof. Using the L -smoothness of F , and the update rules from (4) and (5), the descent lemma of FedGBO with SGDM is given by:

$$F(\mathbf{x}_t) \leq F(\mathbf{x}_{t-1}) - \tilde{\eta} \mathbf{G}_t^\top \mathbf{m}_t + \frac{\tilde{\eta}^2 L}{2} \|\mathbf{m}_t\|^2. \quad (16)$$

Taking expectations of both sides, and inserting Lemma 1 and Lemma 2 into (16):

$$\begin{aligned} \mathbb{E}[F(\mathbf{x}_t)] &\leq \mathbb{E}[F(\mathbf{x}_{t-1})] - \frac{\tilde{\eta}}{2} \sum_{k=0}^{t-1} \beta^k \mathbb{E}[\|\mathbf{G}_{t-k}\|^2] + \frac{\tilde{\eta}Z}{2(1-\beta)} + \frac{2\tilde{\eta}^2 L\beta(R^2 + Z)}{(1-\beta)^3} + \frac{\tilde{\eta}^2 L(R^2 + Z)}{(1-\beta)^2} \\ &= \mathbb{E}[F(\mathbf{x}_{t-1})] - \frac{\tilde{\eta}}{2} \sum_{k=0}^{t-1} \beta^k \mathbb{E}[\|\mathbf{G}_{t-k}\|^2] + \frac{\tilde{\eta}Z}{2(1-\beta)} + \frac{\tilde{\eta}^2 L(1+\beta)(R^2 + Z)}{(1-\beta)^3}. \end{aligned} \quad (17)$$

Rearranging (17), summing over the iterations $t = 1 \dots T$ and telescoping:

$$\frac{\tilde{\eta}}{2} \sum_{t=1}^T \sum_{k=0}^{t-1} \beta^k \mathbb{E}[\|\mathbf{G}_{t-k}\|^2] \leq F(\mathbf{x}_0) - \mathbb{E}[F(\mathbf{x}_T)] + \frac{\tilde{\eta}TZ}{2(1-\beta)} + \frac{\tilde{\eta}^2 LT(1+\beta)(R^2 + Z)}{(1-\beta)^3}. \quad (18)$$

We proceed as [2] do to bound the left hand side of (18). We introduce the change of index $i = t - k$:

$$\begin{aligned} \frac{\tilde{\eta}}{2} \sum_{t=1}^T \sum_{k=0}^{t-1} \beta^k \mathbb{E}[\|\mathbf{G}_{t-k}\|^2] &= \frac{\tilde{\eta}}{2} \sum_{t=1}^T \sum_{i=0}^t \beta^{t-i} \mathbb{E}[\|\mathbf{G}_i\|^2] \\ &= \frac{\tilde{\eta}}{2} \sum_{i=0}^T \mathbb{E}[\|\mathbf{G}_i\|^2] \sum_{t=1}^T \beta^{t-i} \\ &= \frac{\tilde{\eta}}{2(1-\beta)} \sum_{i=1}^T \mathbb{E}[\|\nabla F(\mathbf{x}_{i-1})\|^2] (1 - \beta^{T-i+1}) \\ &= \frac{\tilde{\eta}}{2(1-\beta)} \sum_{i=0}^{T-1} \mathbb{E}[\|\nabla F(\mathbf{x}_i)\|^2] (1 - \beta^{T-i}). \end{aligned} \quad (19)$$

(19) shows a non-normalised iteration probability as defined in Section 4.2 ($\mathbb{P}[t = j] \propto 1 - \beta^{T-j}$). The normalisation constant in order to sum to 1 is:

$$\sum_{i=0}^{T-1} 1 - \beta^{T-i} = T - \beta \frac{1 - \beta^T}{1 - \beta} \geq T - \frac{\beta}{1 - \beta} = \tilde{T}. \quad (20)$$

(19) can then be used in (20) to obtain:

$$\frac{\tilde{\eta}}{2} \sum_{t=1}^T \sum_{k=0}^{t-1} \beta^k \mathbb{E}[\|\mathbf{G}_{t-k}\|^2] \geq \frac{\tilde{\eta}\tilde{T}}{2(1-\beta)} \mathbb{E}[\|\nabla F(\mathbf{x}_t)\|^2]. \quad (21)$$

Inserting (21) into (18), and using the lower bound $F(\mathbf{x}) \geq F^*$ completes the proof:

$$\mathbb{E}[\|\nabla F(\mathbf{x}_t)\|^2] \leq \frac{2(1-\beta)}{\tilde{\eta}\tilde{T}} (F(\mathbf{x}_0) - F^*) + \frac{TZ}{\tilde{T}} + \frac{2T\tilde{\eta}L(1+\beta)(R^2 + Z)}{\tilde{T}(1-\beta)}. \quad \square$$

B Experimental Details

In this section, we provide thorough details about the datasets, models and hyperparameter settings required to reproduce the experiments in the paper. All of the models and algorithms tested were implemented with Pytorch, and run on workstations with Nvidia RTX 2080ti GPUs.

B.1 CIFAR100

A Federated version of the popular CIFAR100 dataset, of (32×32) pixel RGB images from 100 classes. (Reddi et al. 2021) implemented a novel strategy using the Pachinko Allocation Method for distributing the 50,000 training samples in a non-IID fashion among 500 workers, by using the coarse and fine labels associated with each sample. This preprocessed dataset can be downloaded from the Tensorflow Federated library: [tensorflow.org/federated/api_docs/python/tff/simulation/datasets/cifar100](https://www.tensorflow.org/federated/api_docs/python/tff/simulation/datasets/cifar100). Like in similar FL works using this dataset (Reddi et al. 2021) (Karimireddy et al. 2020a) we apply preprocessing composed of a random horizontal flip ($p = 0.5$) followed by a random crop of the (28×28) pixel sub-image, in order to achieve higher test accuracies. This preprocessing is applied by clients during the local training loop of the tested algorithms. The architecture of the CNN model trained on this dataset is given in Table 5. A batch size $B = 32$ was used.

Table 5: Architecture of the CIFAR100 model.

Layer	Activation	Hyperparameters
Convolutional	ReLU	Kernel size = $\{32 \times 3 \times 3\}$, stride = 1
Max Pooling	-	Pool window = $\{2 \times 2\}$
Convolutional	ReLU	Kernel size = $\{64 \times 3 \times 3\}$, stride = 1
Max Pooling	-	Pool window = $\{2 \times 2\}$
Fully Connected	ReLU	Outputs = 512
Fully Connected	Softmax	Outputs = 100

B.2 Sentiment 140

A sentiment-analysis tasking using Twitter posts. This dataset is initially preprocessed using the LEAF federated benchmark tool (Caldas et al. 2019) that groups tweets by the user who posted the tweet, discarding users with < 10 samples, and randomly selecting 20% of each user’s samples to produce a test dataset. We then additionally preprocess this dataset by creating a normalised bag-of-words vector for each sample, using the top 5000 most common tokens in the whole dataset. Each sample is therefore a normalised feature-vector of length 5000, and each target a vector of length two (positive or negative sentiment). We discard all samples that do not contain any of the top 5000 tokens. After this process, we are left with 21876 clients, 336013 total training and 94694 total testing samples. The architecture of the linear model trained on the Sent140 dataset is given in Table 6. The maximum batch size $B = 8$ was used.

Table 6: Architecture of the Sentiment 140 model.

Layer	Activation	Hyperparameters
Fully Connected	Softmax	Outputs = 2

B.3 FEMNIST

A federated version of the EMNIST dataset, containing (28×28) pixel greyscale images from 62 classes. This dataset is preprocessed using the LEAF federated benchmark tool (Caldas et al. 2019), which groups samples by the person who wrote the letter/number in the sample, and randomly selects 20% of each user’s data to produce a pooled test set. We also invert the colours of the samples to produce white-on-black images (like in the classic MNIST dataset). LEAF preprocessing produces a maximum set of 3550 clients, but we take the round number of 3000 clients in all experiments. The architecture of the CNN model trained on this dataset is given in Table 7. A batch size $B = 32$ was used.

B.4 Shakespeare

A next-character prediction task using the complete plays of William Shakespeare. The LEAF (Caldas et al. 2019) preprocessing tool was used to group the lines from all plays by the speaker of the line (e.g. Macbeth, Lady Macbeth, Banquo, etc.). Speakers with < 2 lines were discarded, leaving 660 total clients, lines processed into sequences of length 80, and the last 20% of each speaker’s samples were taken and pooled to create the test set. This preprocessing resulted in a total of 3,678,451 training and 356,921 testing sequences. The architecture of the Gated Recurrent Unit (GRU) model trained on this dataset is given in Table 8. A batch size $B = 32$ was used.

Table 7: Architecture of the FEMNIST model.

Layer	Activation	Hyperparameters
Convolutional	ReLU	Kernel size = $\{32 \times 3 \times 3\}$, stride = 1
Max Pooling	-	Pool window = $\{2 \times 2\}$
Convolutional	ReLU	Kernel size = $\{64 \times 3 \times 3\}$, stride = 1
Max Pooling	-	Pool window = $\{2 \times 2\}$
Fully Connected	ReLU	Outputs = 512
Fully Connected	Softmax	Outputs = 62

Table 8: Architecture of the Shakespeare model.

Layer	Activation	Hyperparameters
Embedding	-	Outputs = 8
Gated Recurrent Unit	{ Sigmoid, Sigmoid, Tanh }	Outputs = 128
Gated Recurrent Unit	{ Sigmoid, Sigmoid, Tanh }	Outputs = 128
Fully Connected	Softmax	Outputs = 79

B.5 Hyperparameter Settings

We now detail the precise combinations of hyperparameter settings used to produce the results presented in Figure 1. For each [dataset, FL algorithm, optimiser] combination we selected the combination of hyperparameters (from a grid-search) that gave the highest test-set accuracy within 5000 communication rounds. As mentioned in section 4.1, for RMSProp and SGDm we searched the parameters $\eta = \{10^1, 10^0, 10^{-1}, 10^{-2}, 10^{-3}, 10^{-4}, 10^{-5}\}$, $\beta = \{0.3, 0.6, 0.9, 0.99, 0.999, 0.9999\}$. For Adam we fixed $\beta_2 = 0.99$ and searched $\beta_1 = \{0.3, 0.6, 0.9, 0.99, 0.999, 0.9999\}$. For RMSProp and Adam we fix $\epsilon = 10^{-3}$ as per (Reddi et al. 2021) and (Karimireddy et al. 2020a). For the AdaptiveFedOpt algorithm we also search local learning rate $\eta_l = \{10^0, 10^{-1}, 10^{-2}, 10^{-3}\}$. When selecting hyperparameters, we discard results that had erratic convergence or diverged part-way through training, as we do not believe these represent desirable, reliable behaviour, even if those settings happened to peak above another hyperparameter combination at one communication round during training. Table 9 gives the hyperparameters for the $K = 10$ experiments shown in Figure 1.

Table 9: Hyperparameter settings used for different [dataset, FL algorithm, optimiser] combinations, using FL algorithm colours: FedGBO, Mimelite, MFL, AdaptiveFedOpt, FedAvg. For RMSProp and SGDm optimisers, $\{\eta, \beta\}$ is given, and for the Adam algorithm, $\{\eta, \beta_1\}$ is presented ($\beta_2 = 0.99$ throughout). For Adam and RMSProp, $\epsilon = 10^{-3}$ throughout. For AdaptiveFedOpt, the local learning rate is also given: $\{\eta, \beta, \eta_l\}$. FedAvg does not use any adaptive optimisation, so only η is presented for each dataset.

Task	$K = 10$		
	RMSProp	SGDm	Adam
CIFAR100	$\{10^{-4}, 0.9\}$	$\{10^{-1}, 0.9\}$	$\{10^{-3}, 0.9\}$
	$\{10^{-3}, 0.99\}$	$\{10^{-2}, 0.9\}$	$\{10^{-4}, 0.9\}$
	$\{10^{-3}, 0.99\}$	$\{10^{-2}, 0.99\}$	$\{10^{-1}, 0.99\}$
	$\{10^{-2}, 0.9, 10^{-2}\}$	$\{10^0, 0.99, 10^{-1}\}$	$\{10^{-2}, 0.9, 10^{-2}\}$
		$\{10^{-2}\}$	
Sent140	$\{10^0, 0.6\}$	$\{10^1, 0.99\}$	$\{10^{-1}, 0.99\}$
	$\{10^0, 0.6\}$	$\{10^1, 0.99\}$	$\{10^{-1}, 0.99\}$
	$\{10^0, 0.6\}$	$\{10^1, 0.99\}$	$\{10^{-1}, 0.99\}$
	$\{10^{-1}, 0.9, 10^0\}$	$\{10^1, 0.9, 10^1\}$	$\{10^{-1}, 0.99, 10^{-1}\}$
		$\{10^1\}$	
FEMNIST	$\{10^{-2}, 0.999\}$	$\{10^{-1}, 0.6\}$	$\{10^{-2}, 0.99\}$
	$\{10^{-2}, 0.999\}$	$\{10^{-1}, 0.9\}$	$\{10^{-2}, 0.99\}$
	$\{10^{-3}, 0.999\}$	$\{10^{-1}, 0.9\}$	$\{10^{-2}, 0.9\}$
	$\{10^{-3}, 0.9, 10^{-1}\}$	$\{10^0, 0.9, 10^{-1}\}$	$\{10^{-2}, 0.6, 10^{-1}\}$
		$\{10^{-1}\}$	
Shakespeare	$\{10^{-3}, 0.9\}$	$\{10^0, 0.9\}$	$\{10^{-3}, 0.6\}$
	$\{10^{-3}, 0.9\}$	$\{10^0, 0.9\}$	$\{10^{-3}, 0.6\}$
	$\{10^{-3}, 0.99\}$	$\{10^0, 0.9\}$	$\{10^{-3}, 0.6\}$
	$\{10^{-2}, 0.6, 10^{-1}\}$	$\{10^0, 0.9, 10^0\}$	$\{10^{-2}, 0.6, 10^{-1}\}$
		$\{10^0\}$	

B.6 Calculation of FLOPs

This section explains the methodology behind calculating the total number of FLOPs required to perform one round of the tested FL algorithms, as shown in Table 4. The computational cost is an important element to consider when choosing an algorithm for a real-world FL deployment: clients are typically low-powered edge devices, such as smartphones, embedded devices, or IoT devices, with limited computational and communication ability. On top of this, the total energy cost of the FL system is an important factor to consider from an environmental perspective (Qiu et al. 2020). Although the total energy cost of running on round of an FL algorithm on a single client is low, the total energy cost over thousands of rounds of training, with thousands of clients participating per round is very large.

The local compute-cost of each algorithm is composed of three parts: the cost of computing K minibatch gradients of size B , the cost of any optimiser-parameter updates that may occur during the local update, and for Mimelite, the cost of computing full-batch gradients. Note that we only calculate the total number of FLOPs from an algorithmic standpoint, and do not consider accelerations such as vectorised operations, as these are dependent on the specific hardware used by clients.

To measure the number of FLOPs required to compute gradients for a single sample for each dataset/model combination, we used the Thop library (<https://github.com/Lyken17/pytorch-OpCounter/>) to compute the total number of FLOPs for a single forward pass. Using the general formula from the ‘‘AI and Compute’’ blog from OpenAI (<https://openai.com/blog/ai-and-compute/>), we multiplied the value produced by the Thop library by 3 in order to get the total FLOPs for a single forward-backward pass on one sample.

Calculating the FLOPs required for local adaptive optimisation requires taking the number of parameters of each model, and multiplying this number by the total number of operations given by the optimisation algorithm, plus any local optimiser updates that occur. For example, for the FedGBO and Mime algorithms using RMSProp, inspection of Table 1 shows that there are 4 operations per step that act on either \mathbf{g} or \mathbf{v} (multiplication by $-\eta$, division of $-\eta\mathbf{g}$, square-rooting \mathbf{v} , and addition of ϵ to $\sqrt{\mathbf{v}}$). For MFL using RMSProp, there are 7 operations, the 3 operations in the tracking step \mathcal{T} followed by the 4 operations in \mathcal{U} . For the SGDm optimiser, however, FedGBO, Mime and MFL all have 4 operations per model update, as the \mathcal{T} step, used to update \mathbf{m} locally in MFL, can be directly applied to the local model update without extra operations. The FedAvg and AdaptiveFedOpt algorithms both use vanilla SGD on clients, so have 2 operations per model update (multiplication of \mathbf{g} by η followed by subtraction).

Finally, for the Mimelite algorithm, the computation of full-batch gradients requires multiplying the total number of operations for computing one forward-backward pass by the average number of samples per client. The formulas for computing the FLOPs for the local update of each algorithm, N are therefore as follows:

$$N_{\text{FedGBO}} = K(B(\text{fwd} + \text{bwd}) + C_{\text{FedGBO}}|\mathbf{x}|), \quad (22)$$

$$N_{\text{Mimelite}} = K(B(\text{fwd} + \text{bwd}) + C_{\text{FedGBO}}|\mathbf{x}|) + n(\text{fwd} + \text{bwd}), \quad (23)$$

$$N_{\text{MFL}} = K(B(\text{fwd} + \text{bwd}) + C_{\text{MFL}}|\mathbf{x}|), \quad (24)$$

$$N_{\text{AdaptiveFedOpt}} = K(B(\text{fwd} + \text{bwd}) + 2|\mathbf{x}|), \quad (25)$$

$$N_{\text{FedAvg}} = K(B(\text{fwd} + \text{bwd}) + 2|\mathbf{x}|), \quad (26)$$

$$(27)$$

where K is the number of local updates, B is the minibatch size, fwd and bwd are the FLOPs required to compute the forward and backward passes of the model on one sample, C_* is the number of operations associated with the variant of local adaptive optimiser used (as discussed above), $|\mathbf{x}|$ is the total number of model parameters, and n is the average number of client samples, as shown in Table 3. B and $|\mathbf{x}|$ for each dataset are given in Appendix B.1-B.4, the C_* values given in Table 10 below, and n for each dataset is given in Table 3.

Table 10: Number of operations per local step of FedGBO and Mimelite algorithms.

Algorithm	C_{FedGBO}	C_{MFL}
RMSProp	4	7
SGDm	4	4
Adam	7	10